Received: 24 February 2019 | Revised: 12 July 2019 | Accepted: 13 July 2019

DOI: 10.1002/term.2936

RESEARCH ARTICLE

WILEY

A comparison study of different decellularization treatments on bovine articular cartilage

Toktam Ghassemi[1] | Nasser Saghatoleslami[1] | Nasser Mahdavi-Shahri[2] | Maryam M. Matin[2] | Reza Gheshlaghi[1] | Ali Moradi[3]

[1] Department of Chemical Engineering, Ferdowsi University of Mashhad (FUM), Mashhad, Iran

[2] Department of Biology, Ferdowsi University of Mashhad (FUM), Mashhad, Iran

[3] Orthopedic Research Center, Mashhad University of Medical Sciences, Mashhad, Iran

Correspondence
Ali Moradi, Bone and Joint Research Lab, Library Building, Ghaem Hospital, Shariati Square, Mashhad, Iran.
Email: ralimoradi@gmail.com

Funding information
Ferdowsi University of Mashhad, Grant/Award Numbers: 3/27432-11/03/1392 and #3/27432-11/03/1392; Mashhad University of Medical Sciences, Grant/Award Numbers: 960363-06/10/1396 and #960363-06/10/1396

Abstract

Previous researches have emphasized on suitability of decellularized tissues for regenerative applications. The decellularization of cartilage tissue has always been a challenge as the final product must be balanced in both immunogenic residue and mechanical properties. This study was designed to compare and optimize the efficacy of the most common chemical decellularization treatments on articular cartilage. Freeze/thaw cycles, trypsin, ethylenediaminetetraacetic acid (EDTA), sodium dodecyl sulfate (SDS), and Triton-X 100 were used at various concentrations and time durations for decellularization of bovine distal femoral joint cartilage samples. Histological staining, scanning electron microscopy, DNA quantification, compressive strength test, and Fourier-transform infrared spectroscopy were performed for evaluation of the decellularized cartilage samples. Treatment with 0.05% trypsin/EDTA for 1 day followed by 3% SDS for 2 days and 3% Triton X-100 for another 2 days resulted in significant reduction in DNA content and simultaneous maintenance of mechanical properties. Seeding the human adipose-derived stem cells onto the decellularized cartilage confirmed its biocompatibility. According to our findings, an optimized physiochemical decellularization method can yield in a nonimmunogenic biomechanically compatible decellularized tissue for cartilage regeneration application.

KEYWORDS

articular cartilage, chemical detergents, decellularization, extracellular matrix (ECM), optimization, tissue engineering

1 | INTRODUCTION

Articular cartilage has a limited intrinsic ability for regeneration after injury due to its avascular and aneural properties (Marcacci, Filardo, & Kon, 2013). Arthritis is the leading cause of disability worldwide. Aging, genetic predisposition, abnormal biomechanics, obesity, and trauma impact the disease process. Comorbidities like cardiovascular diseases, metabolic syndrome, and diabetes can worsen the condition (Bijlsma, Berenbaum, & Lafeber, 2011; Blanco & Ruiz-Romero, 2012; Conaghan, 2013; Henrotin, 2014). Untreated lesions lead to debilitating joint pain, dysfunction, and osteoarthritis (Manek & Lane, 2000). Filling the void with a biomechanically compatible tissue and successful integration of the repaired and the native cartilage are two major concerns in cartilage regeneration (Redman, Oldfield, & Archer, 2005). None of the routine conventional approaches has been the ultimate choice for treatment of articular chondral lesions. Tissue engineering strategies introduce combinations of cells, biomaterial scaffolds, and growth factors to fabricate proper alternatives for cartilage tissue (Valiani et al., 2014). Recently, extracellular matrix (ECM)-derived scaffolds have been suggested to possess chondroinductive properties (Moradi, 2015; Moradi et al., 2014; Moradi et al., 2016; Sutherland, Converse, Hopkins, & Detamore, 2015). The ECM content

and architecture are simultaneously preserved in decellularized tissue. Decellularization treatments are particularly necessary with xenogeneic scaffolds as host immune response may be arisen by residual DNA, alpha-Gal epitope, or human leukocyte antigens (Sutherland, Converse, et al., 2015). Basically, cartilage decellularization is performed through diffusion of detergents into the lacunas to lysate the chondrocytes followed by washing out the debris and genetic material. The process comprises a combination of physical, chemical, and enzymatic steps. Cartilage decellularization is an important challenge due to its dense structure (Gong et al., 2011). Various procedures have been suggested to improve the diffusion of the detergent into the tissue through fine fragmentation of the sample (Yang et al., 2008) into powder (Yang et al., 2010) or microlayers (Gong et al., 2011). In addition to specific ECM biomolecules, articular cartilage has a special zonal 3D structure that supports its mechanical properties. Although fine processing yields in better detergent penetration, it demolishes the unique multiphase architecture of the articular cartilage. As an alternative strategy, decellularization without tissue homogenization can preserve cartilage architecture, while alleviating the immunologic and xenogeneic concerns. The current study has been designed to present an easy, optimized, and practical decellularization procedure capable of maximal preservation of the zonal columnar organization of the intact articular cartilage and simultaneously, minimal diminution in its biochemical properties.

2 | MATERIALS AND METHODS

2.1 | Tissue harvest

Bovine femur bones were collected from local abattoir immediately after separation from 6- to 12-month-old calves (n = 11), kept wet in phosphate-buffered saline (PBS; Merck, Germany) and transferred to the laboratory. The articular cartilage was manually dissected from the patellar groove using microtome sharp blades (Leica, Germany) then punched by a 10-mm metallic puncher (AMKA, Japan). The samples were washed with PBS, covered in PBS-wetted gauze, and stored in −20°C freezer until further processing (Kheir et al., 2011; Peretti, Randolph, Villa, Buragas, & Yaremchuk, 2000).

2.2 | Decellularization

The decellularization process was performed in three phases. According to the previous studies (Gilbert, 2012; Kheir et al., 2011), freeze/thaw cycles were followed by either one or combinations of two or more chemical/enzymatic procedures: trypsin (Benders et al., 2014; Toolan, Frenkel, Pereira, & Alexander, 1998; Yang et al., 2010; Zheng et al., 2011), ethylenediaminetetraacetic acid (EDTA; Yang et al., 2008, Jia et al., 2012, Kang et al., 2014), Triton X-100 (Chang et al., 2014; Moradi et al., 2014; Sutherland et al., 2015; Yang et al., 2008; Zheng et al., 2011), and sodium dodecyl sulfate (SDS; Elder, Eleswarapu, & Athanasiou, 2009; Kheir et al., 2011; Gong et al., 2011). Initially, 14 methods were designed as the screening step according to the previous studies to define the efficacy as well as the interaction between the agents (Table 1). Freeze/thaw cycles (2-min freezing in liquid nitrogen at −196°C followed by 3-min thawing in 50-ml falcon tubes in tap water at room temperature) were repeated 5 times for all samples before starting each procedure (Kheir et al., 2011). A separate set of samples (blanks) were exposed to only PBS to elucidate its effect on decellularization. Also, another set of samples were kept untouched at −20°C freezer as the control group (C). All solutions were prepared using PBS. All washing steps were done in a shaker incubator at 200 rpm, 37°C. All samples were finally washed with PBS for 24 hr. The scoring was performed based on the nucleus state and presence of debris in the lacunas in staining (Table 2). The sample size for microscopy pictures was between 3 and 5 slides per sample. Two pathologists independently scored the samples according to the previous reports, and a consensus was achieved through discussion in case of any mismatch. Based on the scores from Phase 1, the possible schemes were designed for the second phase of optimization as shown in Table 3.

TABLE 1 Reagent combination and timing schedule of cartilage decellularization in Phase 1

Procedure	Day 1	Day 2	Day 3	Day 4
1	0.1% EDTA	0.1% EDTA	2% Triton X-100	2% Triton X-100
2	0.1% EDTA	0.1% EDTA	2% SDS	2% SDS
3	2% Triton X-100	2% Triton X-100	2% SDS	2% SDS
4	0.1% EDTA	2% Triton X-100	2% SDS	2% SDS
5	0.25% trypsin	0.1% EDTA	0.1% EDTA	0.1% EDTA
6	0.25% trypsin	1% Triton X-100	1% Triton X-100	1% Triton X-100
7	0.25% trypsin	2% Triton X-100	2% Triton X-100	2% Triton X-100
8	0.25% trypsin	1% SDS	1% SDS	1% SDS
9	0.25% trypsin	2% SDS	2% SDS	2% SDS
10	0.25% trypsin	0.1% EDTA	2% Triton X-100	2% Triton X-100
11	0.25% trypsin	0.1% EDTA	2% SDS	2% SDS
12	0.25% trypsin	1% Triton X-100	1% SDS	1% SDS
13	0.25% trypsin	2% Triton X-100	2% SDS	2% SDS
14	0.25% trypsin	0.1% EDTA	2% Triton X-100	2% SDS
Blank	PBS	PBS	PBS	PBS
C	—	—	—	—

Abbreviations: EDTA, ethylenediaminetetraacetic acid; PBS, phosphate-buffered saline; SDS, sodium dodecyl sulfate.

TABLE 2 Scoring table for AC decellularization index, based on lacuna and nucleus state (bar, 2 μm)

Score	State	Schematic
0	Intact nucleus	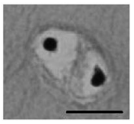
1	Deformed nucleus	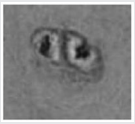
2	Dissolved nucleus + full of debris lacunas	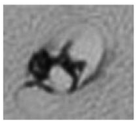
3	Dissolved nucleus + mainly filled lacunas	
4	Dissolved nucleus + partially filled lacunas	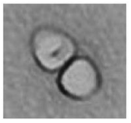
5	Dissolved nucleus + clear lacunas	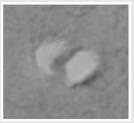

According to the results in Phase 2, Phase 3 of experiments was designed for evaluation of complete debris elimination (Table 4).

2.3 | DNA content

Nontreated and decellularized cartilage samples (n = 5 in each group) were finely fragmented. Briefly, the cartilage samples were snap frozen in liquid nitrogen and fined in a metallic laboratory pulverizer and a hammer. The pulverized cartilage was moved into the DNA preservation buffer. DNA quantification was performed using the Genomic DNA isolation kit (kit-I (25) #S-1030, DENAzist, Iran) according to the manufacturer's protocol through absorbance measurement at 260/280 nm using a Nanodrop spectrophotometer (Thermo Fischer Scientific, USA).

2.4 | Fourier-transform infrared spectroscopy

The lyophilized samples were pulverized into fine powder with potassium bromide (KBr). The powder was press fit into a mold. The reflection Fourier-transform infrared (FTIR) data were collected at 4-cm^{-1} spectral resolution (Thermo Nicolet, USA) in the wavenumber region between 4,000 and 400 cm^{-1}.

2.5 | Biomechanical analysis

The mechanical properties of nontreated and decellularized articular cartilage punches were analyzed on a mechanical testing machine (SANTAM, Iran). Samples were transferred to a dish-containing PBS equilibrated to room temperature. They were individually tested under unconfined compression by an impermeable 5-cm diameter indentor. A constant compressive strain rate of 100 μm/min was applied until ~60% of maximal deformation was achieved, and a stress-strain curve was generated. Young's modulus of the tested tissue was calculated based on the initial linear slope of the stress–strain curve.

2.6 | Water content

The water content of nontreated and decellularized samples was quantitatively determined by a previously reported formula (Im, Li, Wang, Zhang, & Keidar, 2012). Briefly, fresh samples from each group were placed on a filter paper for 1 min to eliminate excess water then weighed before (W_{wet}) and after (W_{dry}) freeze drying for 24 hr (Moradi, Pramanik, Ataollahi, Abdul-Khalil, et al., 2014). The water content was defined as the ratio of the weight decrease ($W_{wet} - W_{dry}$) to the initial weight (W_{wet}; Moradi, 2015):

TABLE 3 Design of decellularization experiments for bovine articular cartilage in Phase 2

Method number	1	2	3	4	5	6	7	8	9	10	11	12	13	14	15	16	17
Freeze/thaw cycles	¶	6	0	6	0	6	0	6	0	6	0	6	0	6	0	6	3
Trypsin/EDTA	¶	-	+	+	-	-	+	+	-	-	+	+	-	-	+	+	§
Triton-X100	¶	-	-	-	+	+	+	+	-	-	-	-	+	+	+	+	§
SDS	¶	-	-	-	-	-	-	-	+	+	+	+	+	+	+	+	§

Abbreviations: EDTA, ethylenediaminetetraacetic acid; SDS, sodium dodecyl sulfate.

¶Not processed (C).

-Phosphate-buffered saline.

+Solutions; 0.05% for trypsin/EDTA and 3% for Triton-X100 and SDS.

§Solutions with half concentration as center point; 0.025% for trypsin/EDTA and 1.5% for Triton-X100 and SDS.

TABLE 4 Decellularization methods design in Phase 3 of experiments

Method number	Day 1	Day 2	Day 3	Day 4	Day 5
1	0.05% trypsin/EDTA	3% SDS	3% Triton X-100	—	—
2	0.05% trypsin/EDTA	3% SDS	3% SDS	—	—
3	0.05% trypsin/EDTA	3% SDS	3% SDS	3% Triton X-100	—
4	0.05% trypsin/EDTA	3% SDS	3% Triton X-100	3% Triton X-100	—
5	0.05% trypsin/EDTA	3% SDS	3% SDS	3% Triton X-100	3% Triton X-100

Abbreviations: EDTA, ethylenediaminetetraacetic acid; SDS, sodium dodecyl sulfate.

$$\text{Water Content} = \frac{(W_{\text{wet}} - W_{\text{dry}})}{W_{\text{wet}}} \times 100.$$

2.7 | Biocompatibility

Biocompatibility tests are necessary to confirm the safety of decellularization in terms of possible hazards of chemical and reagent residues. Human adipose-derived stem cells (hADSCs) were obtained from redundant subcutaneous abdominal adipose tissue through cosmoplastic surgery following a published protocol (Bahrami et al., 2011). The clearance to conduct this study was provided by Ferdowsi University of Mashhad Ethics Committee (#3/27432-11/03/1392). The hADSCs were cultured in Dulbecco's modified Eagle's medium (DMEM; Gibco, USA) supplemented with 10% fetal bovine serum (Gibco, USA) and 1% penicillin–streptomycin (Biowest, UK) at 37°C in 5% CO2 during expansion. The media was changed every other day. Subculturing was performed at 90% confluency using 0.05% trypsin. The cells were harvested at Passage 3, counted, resuspended in culture medium at 5×10^5 cells per 300 µl, and seeded onto both sides of the sterilized decellularized cartilage discs (Rowland, Colucci, & Guilak, 2016). The constructs were individually placed in 24-well plates (Orange Scientific, France) and incubated at 37°C for 1 hr for cell attachment before adding 1 ml of culture medium in each well. The medium was changed every 2–3 days. Cell growth and viability were checked at Days 7 and 14 through hematoxylin and eosin (H&E) staining.

2.8 | Histology

The cartilage constructs were fixed in formalin, dried in serial dilutions of ethanol, embedded in paraffin, sectioned at a thickness of 7 µm, and stained with H&E for histological analyses: DAPI for nucleus revelation, picrosirius red (PR) for collagen content, and toluidine blue (TB) for glycosaminoglycan (GAGs) content according to previously described protocols (Schmitz, Laverty, Kraus, & Aigner, 2010).

2.9 | Scanning electron microscopy

The decellularized cartilage samples were rinsed overnight in deionized water at 37°C in a shaker incubator with several water changes and freeze-dried for 24 hr (Heto, Denmark). Samples were gold–palladium coated after dehydration and examined on a SEM (LEO 1450VP, Germany).

2.10 | Statistical analysis

All data were expressed as mean ± standard deviation. Student's *t* test was used to determine the statistical significance between groups. A $p < .05$ was considered as statistically significant.

3 | RESULTS

3.1 | Decellularization procedure

Figure 1a displays the histological results of Phase 1. Extensive staining of the chondrocytes nuclei was observed in the control group whereas the blank samples subjected to PBS showed nuclei shrinkage, indicating no decellularization. The decellularization scores for each procedure are shown in Figure 1b. Procedures 10, 11, 13, and 14 resulted in the highest scores with almost no nuclei or cell debris. The treatments started with EDTA failed even to deform the nuclei, whereas trypsin dissolved almost the entire nuclei.

The EDTA in combination with trypsin resulted in better cell debris wash out compared with trypsin alone in Procedures 10, 11, and 14. Although the decellularization process was incomplete without trypsin, high concentrations of trypsin (≥0.25%) resulted in a loose gel-like tissue (Benders et al., 2014).

The second phase of experiments was designed in order to optimize trypsin/EDTA and consequently, detergent concentration (0.05% and 3%, respectively; Zheng et al., 2011). Freeze/thaw cycles did not show any effect on lacuna clearance.

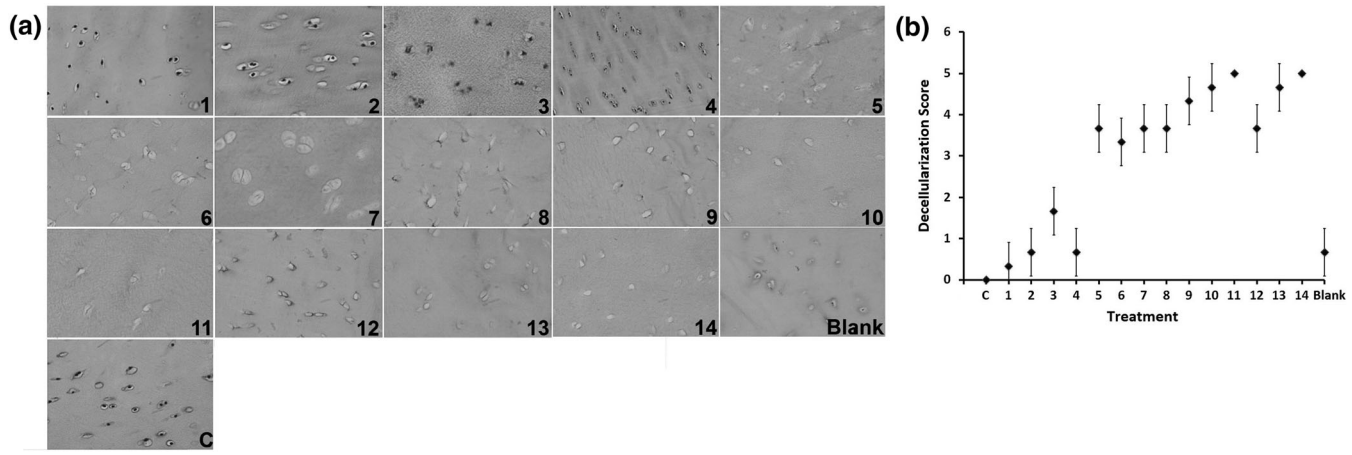

FIGURE 1 (a) Hematoxylin staining photomicrographs demonstrating construct cellularity of articular cartilage middle zone for various treatment groups in Phase 1. Treatments with 0.25% trypsin decreased cellularity and Procedures 10, 11, 13, and 14 eliminated almost all nuclei and cell debris (bar, 10 μm). (b) Decellularization scores for all 14 treatments in Phase 1, based on Table 2 (n = 5)

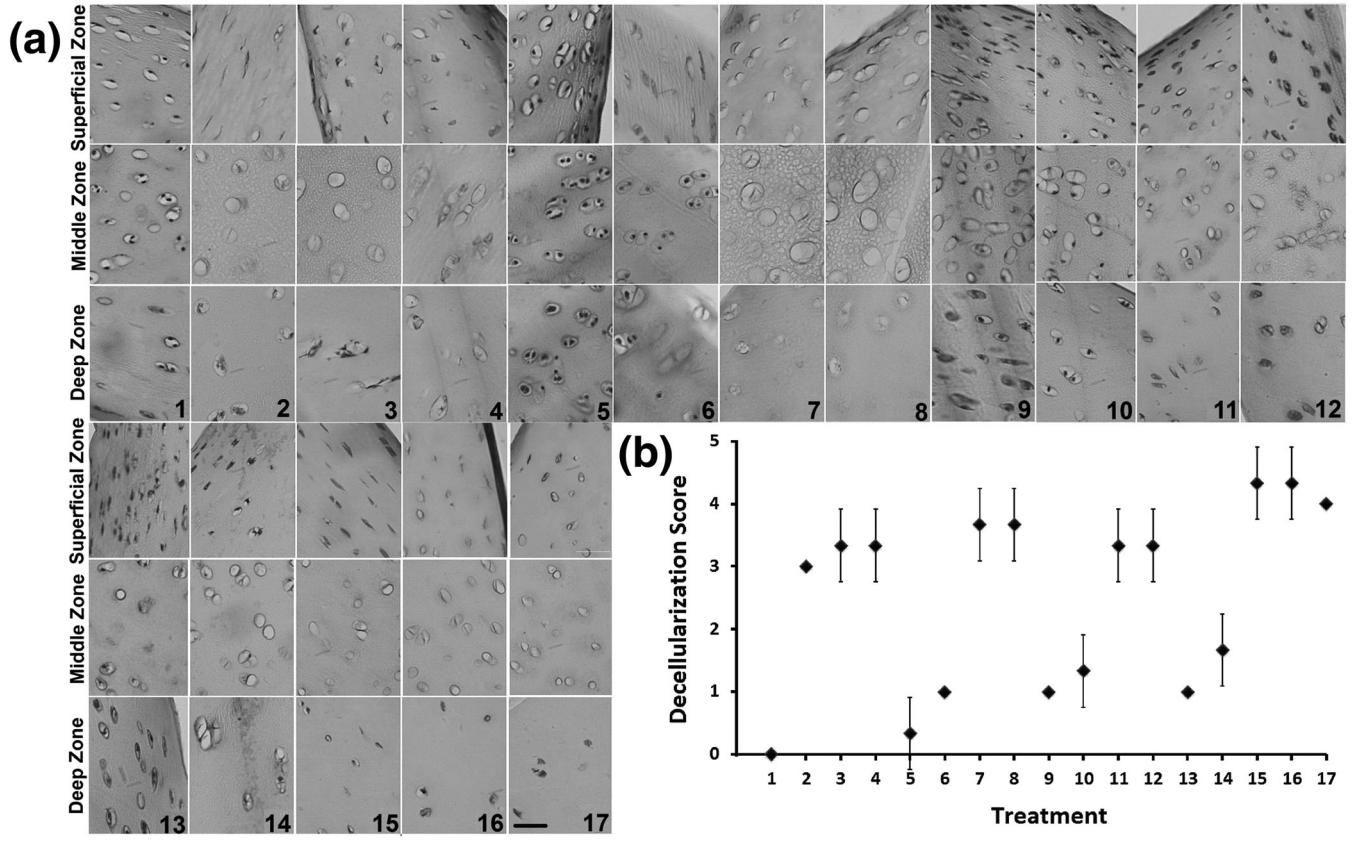

FIGURE 2 (a) Micrographs of hematoxylin stained decellularized bovine articular cartilage in different zones at Phase 2. Nucleus dissolution was seen in some procedures like 15, but no treatments resulted in complete elimination of cell debris (bar, 50 μm). (b) Decellularization scores in Phase 2, based on Table 2 (n = 5)

Figure 2a depicts the digital images of histological staining in Phase 2. The decellularization scores for each method at each zone (superficial, middle, and deep) are shown in Figure 2b.

Procedures 15 and 16 resulted in the highest decellularization scores; however, as none of the procedures resulted in complete decellularization in all three zones, the exposure time was extended in the final phase. Figure 3a displays the results of H&E staining in Phase 3. The decellularization scores for each procedure are shown in Figure 3b.

Although the nuclei were demolished in all groups, only the fifth method (Day 1: 0.05% trypsin/EDTA; Days 2–3: 3% SDS; days 4–5: 3% Triton X-100) histologically resulted in almost complete

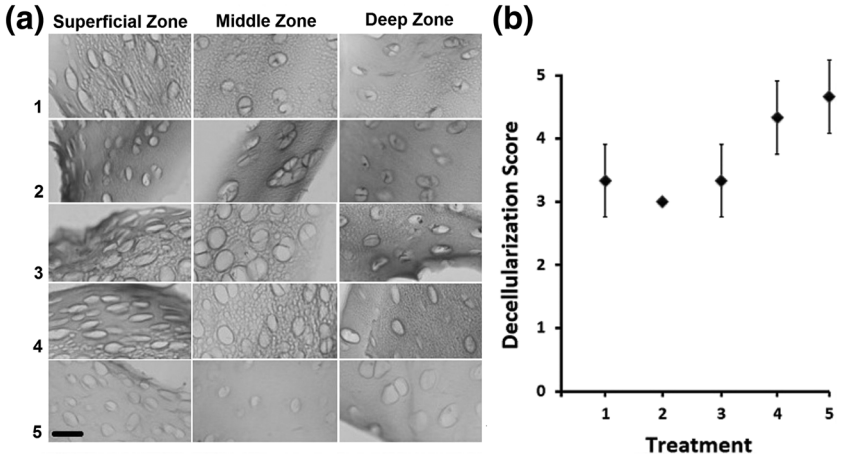

FIGURE 3 (a) Micrographs of hematoxylin and eosin-stained decellularized bovine articular cartilage in different zones through Phase 3 of experiments (bar, 20 μm); (b) the effect of different treatments with extended times on decellularization of articular cartilage (n = 5)

decellularization, but clearly empty lacunas were not seen in all zones with other formulas.

3.2 | Morphology and histology

Figure 4a shows the macromorphology and surface appearance of intact and decellularized cartilage samples. Whereas nontreated samples appeared milky white discs (10 mm in diameter and 1.27 ± 0.20 mm in thickness) with a hard texture, the decellularized samples were transparent and soft (Schwarz et al., 2012). Although lyophilization decreased the thicknesses in both nontreated and treated samples, however, no change in diameter was seen.

The SEM micrographs (Figure 4b–d) depict the zonal structure of the highly porous cartilage samples.

The H&E staining resulted in completely clear lacunas. Also, no nucleus was observed in DAPI staining (Figure 5). The PR and TB staining indicated the presence of the collagen and sulfated proteoglycan (GAGs), respectively, in ECM. No noticeable changes in collagen content were seen in PR-stained decellularized cartilage compared with the intact samples. However, TB staining proved that

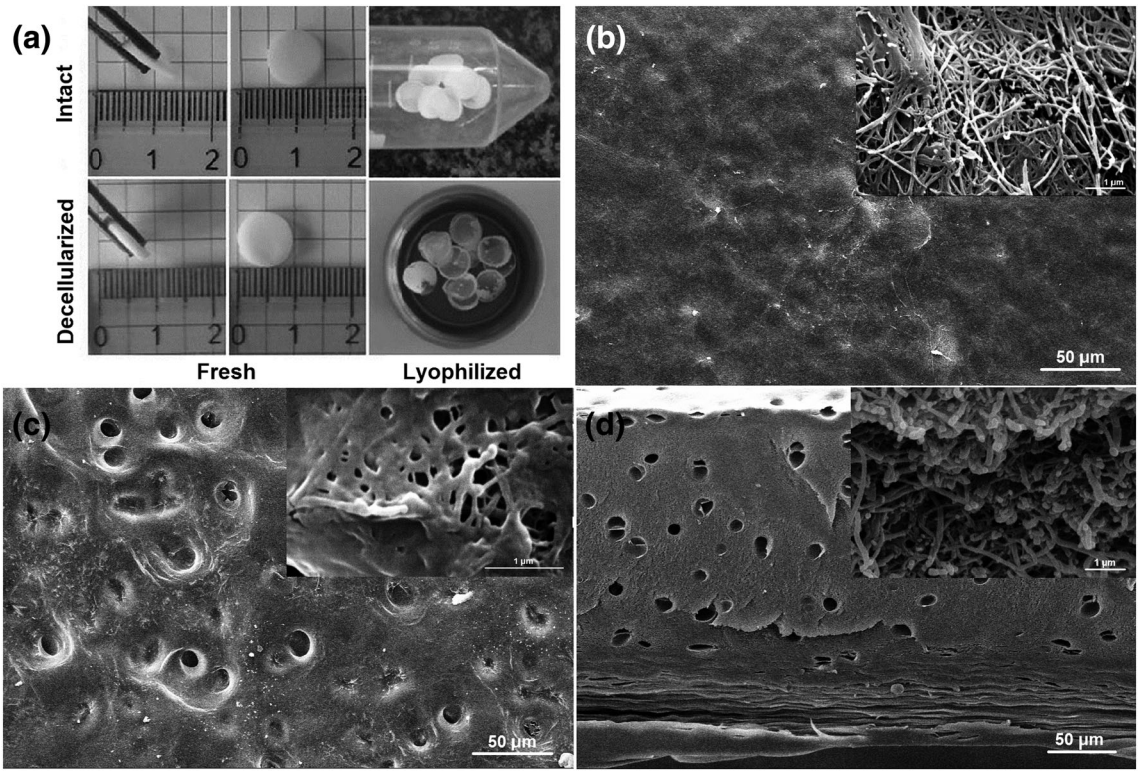

FIGURE 4 Scanning electron microscopy micrographs of (a) dimensions and gross morphology of intact (nontreated) and decellularized articular cartilage discs, (b) superficial, (c) deep, and (d) cross-sectional zones of decellularized bovine articular cartilage (the inset pictures have been rendered at high magnifications)

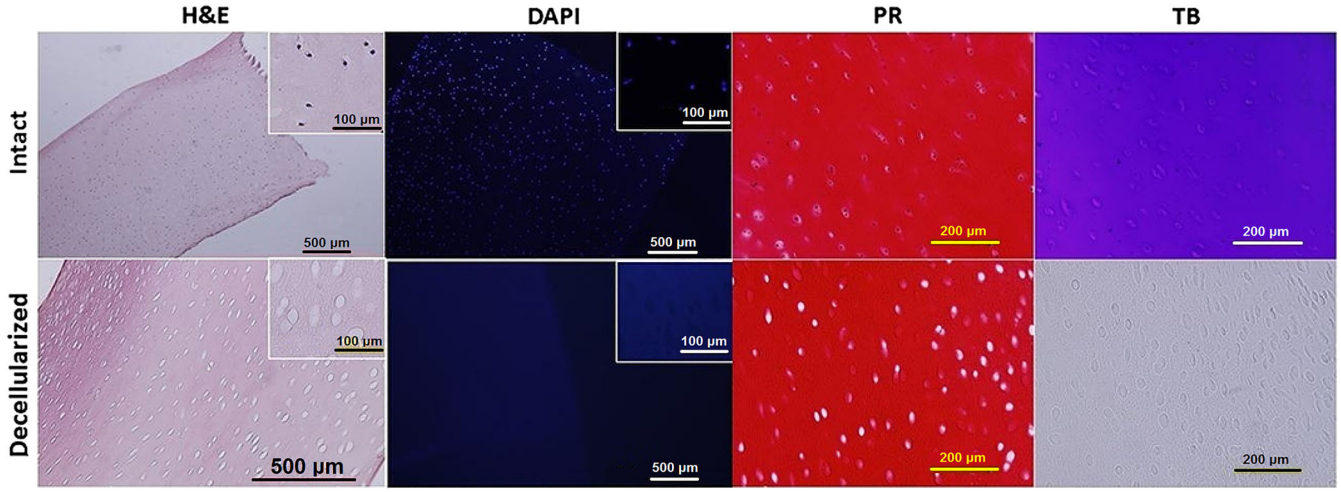

FIGURE 5 Photomicrographs demonstrating cellularity (hematoxylin and eosin [H&E] and DAPI), collagen content (picrosirus red [PR]), and GAGs content (toluidine blue [TB]) for control (intact) and treatment (decellularized) groups. Selected decellularization protocol eliminated all nuclei while preserving collagen content, but eliminated GAGs [Colour figure can be viewed at wileyonlinelibrary.com]

most of the GAGs has been washed out during the decellularization treatment.

3.3 | DNA content

Decellularization resulted in a significant reduction (77%) in DNA content (262 ± 42 ng/mg) compared with the nontreated cartilage sample (1,146 ± 93 ng/mg; $p < .05$; Figure 6a).

3.4 | FTIR spectroscopy

The FTIR spectra of intact and decellularized bovine cartilage are shown in Figure 6b. The absorbance bands of decellularized cartilage matched that of the intact samples, confirming that the treatment has not altered the chemical composition of cartilage ECM; however, the band ratios changed.

3.5 | Biomechanical testing

Young's modulus in decellularized samples (0.55 ± 0.15 MPa) showed a nonsignificant decrease in comparison with the intact ones (0.36 ± 0.07 MPa; $p = .1$; Figure 6c).

3.6 | Water content

No significant difference was seen in water content between the intact (90 ± 19%) and decellularized (82 ± 42%) specimens ($p = .81$).

3.7 | Biocompatibility

The H&E staining showed hADSCs cell proliferation on decellularized cartilage at Days 7 and 14 (Figure 6d). The deep zone showed a better cell penetration due to its proportionally bigger pore sizes compared with the superficial zone. However, the dense compact reticular fibrous nature of the decellularized cartilage restricted cell penetration and hence, can be the most considerable limitation of application in recellularization.

4 | DISCUSSION

Tissue-derived decellularized constructs are believed to be potential substitutes for tissue regeneration. However, feasible cost-effective reproducible methods for decellularization of various tissues are yet to be optimized. In this study, cartilage decellularization protocols using the common available detergents were evaluated. Our optimized method (Day 1: 0.05% trypsin/EDTA; Days 2–3: 3% SDS; Days 4–5: 3% Triton X-100) resulted in almost complete decellularization of bovine articular cartilage.

Considering the low number of isotype calves slaughtered, a relatively low sample size was the major limitation for this study, especially for the early screening experiments. Also, although staining has reportedly been referenced as the common acceptable method for evaluation of decellularization (Crapo, Gilbert, & Badylak, 2011), quantitative tests like DNA (i.e., Hoechst 33258), Collagen II (ELISA), and GAGs (DMMB method) measurements could have reconfirmed our results; however, time and budget restrictions have always been substantial obstacles for research. Also, decellularization chemistry has shown to change the tissue molecular structure and affect mass transferring and cell response (Moore, Sarntinoranont, & Mcfetridge, 2012). The risk of residual chemicals is another problem with decellularization; for example, SDS has a high affinity for proteins (Grefrath & Reynolds, 1974), eliminates ECM growth factors (Reing et al., 2010), and leads to incomplete decellularization (Mendoza-Novelo & Cauich-Rodríguez, 2011; Rémi et al., 2011), ECM retention (Arai & Orton, 2009; Kawazoye et al., 1995; Knight, Wilcox, Korossis, Fisher, & INgham, 2008), and calcification (Jorge-Herrero et al., 1994).

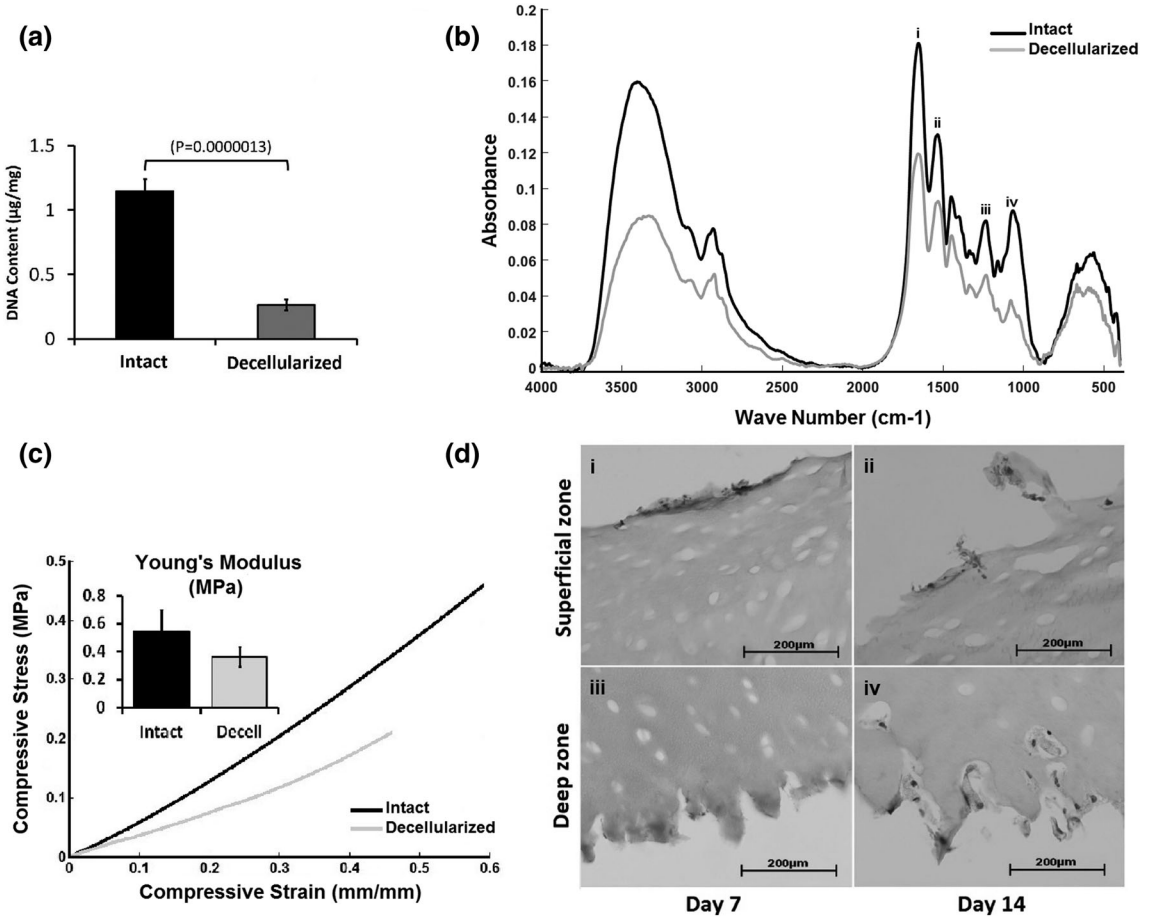

FIGURE 6 (a) DNA content in intact and decellularized bovine articular cartilage (n = 5). (b) Typical Fourier-transform infrared absorption spectra of intact and decellularized bovine articular cartilage (n = 3): i, amide I (1,585-1,720 cm^{-1}); ii, amide II (1,500–1,585 cm^{-1}); iii, amide III (1,200–1,300 cm^{-1}); and iv, carbohydrate region (985–1,140 cm^{-1}). (c) The representative compressive stress/strain curves for intact and decellularized bovine articular cartilage with the corresponding Young's moduli (n = 5). (d) Representative images of hematoxylin and eosin-stained human adipose-derived stem cells seeded on superficial (i and ii) and deep zones (iii and iv) of decellularized cartilage at Days 7 (i and iii) and 14 (ii and iv)

Demolition of ECM components will result in deterioration of the mechanical properties of the tissue (Elder et al., 2009).

Consistent with a previous report, the effective concentrations of Triton-X and SDS in our study were at 3% (Zheng et al., 2011). Although freeze/thaw cycles have been used in a previous study for facilitation of cell wall diffusion, we found that these cycles have no significant benefits when enzymatic digestion is performed (Kheir et al., 2011).

Also, according to our findings, SDS was found to be superior to Triton X-100 in terms of permeability (Elder et al., 2009). No shrinkage in the sample diameter was observed after decellularization as reported by a previous study (Luo, Eswaramoorthy, Mulhall, & Kelly, 2016).

Collagen preservation and GAGs elimination as the results of decellularization in our study were congruent with the findings of the previous studies (Crapo et al., 2011; Gilbert, Sellaro, & Badylak, 2006; Kheir et al., 2011; Toolan et al., 1998).

Several decellularization protocols for articular cartilage have been suggested in recent years; however, the acceptable level of the residual genetic material in decellularized tissues remains controversial (Graham, Gratzer, Bezuhly, & Hong, 2016). The lower DNA washout (77%) in our suggested protocol compare with 88% reported by Lue et al. (2016) can be due to hyaluronidase treatment in their study.

The decellularized bovine cartilage showed a nonsignificant (p = .1) decrease in its compressive strength (0.36 ± 0.07 MPa) in comparison with the intact cartilage (0.55 ± 0.15 MPa). The result can be attributed to the variance of the sample sources. The SDS treatment for 6 hr has been shown to reduce Young's modulus in engineered articular cartilage constructs (Elder et al., 2009). A significant decrease has been also reported in the equilibrium (~90%) and dynamic (~60%) moduli of the porcine articular cartilage subjected to several freeze–thaw cycles and hyaluronidase treatment (Luo et al., 2016). This decrease can be due to possible disruption of collagen network through crystal formation in freeze–thaw cycles (Badylak, 2007; Badylak, Freytes, & Gilbert, 2009). It seems that the efficacy of decellularization is reversely correlated with the mechanical properties of the samples. Gentle protocols are more likely to result in incomplete removal of DNA, while

preserving the mechanical properties of the samples; however, a more coarse protocol might lead to less DNA residue with a diminished mechanical strength.

The infrared absorption spectrum of articular cartilage is mainly created by collagen and GAGs absorption, with a collagen dominancy (Muir, 1980). Amide I and II regions (≈1,585–1,720 cm^{-1} and ≈1,500–1,585 cm^{-1}, respectively) have the strongest infrared absorptions (Saarakkala, Rieppo, Rieppo, & Jurvelin, 2010). An almost 10% decrease was seen in the ratio of amides to each other (amide I/amide II and amide III/amide II), whereas the ratio of GAGs to each amide group (GAGs/amide I, GAGs/amide II, and GAGs/amide III) showed a more than 30% decline. These changes in the ratios can be attributed to a proportionally bigger GAGs loss in the decellularization treatment compared with collagen, as reported in a similar study (Luo et al., 2016).

The results of water content measurement was in line with the results of a previous study (85–90%) for bovine knee joints articular cartilage (Yang et al., 2010); however, another study had reported the water content in bovine metacarpophalangeal articular cartilage to be less than 70% (Moradi, 2015; Moradi, Pramanik, Ataollahi, Khalil, et al., 2014).

No noticeable difference was observed in cell proliferation between the superficial and deep zones due to the similar biochemical and nanostructural environment. However, compact horizontal collagen fibers in superficial zone restricted cell penetration.

Although the decellularization processing led to a significant loss in the DNA and a noticeable decrease in GAGs contents, the resulting tissue preserved its mechanical properties and biocompatibility. As a main criterion, the DNA content in decellularized tissue has been defined to be less than 50 ng/mg of DNA/dry ECM; however, the dense compact nature of the reticular network of fibrous ECM in cartilage is a substantial barrier for the detergents to penetrate into as well as the nucleic material to be washed out (Graham et al., 2016). This can be mentioned as a major limitation in application of the decellularized cartilage tissue.

Due to inferior mechanical properties of decellularized bovine (0.55 ± 0.15 MPa) to human articular cartilage (0.84–3.0 MPa; Izadifar, Chen, & Kulyk, 2012), supplementary treatments are needed to compensate the mechanical strength of decellularized cartilage constructs. Once complete chemical detergents removal has been ensured, in vivo studies should be performed to determine the immune response to the decellularized tissue. In addition to reduction in cellularity, investigation on the elimination of the Galα1,3 epitope should be performed to avoid hyperacute rejection of xenografts (Platt et al., 1991).

ACKNOWLEDGMENTS

The authors would like to acknowledge financial support from the Ferdowsi University of Mashhad (#3/27432-11/03/1392), Mashhad University of Medical Sciences (#960363-06/10/1396), Mashhad, Iran, and Clinical Research Unit, Qaem Hospital, Faculty of Medicine, Mashhad University of Medical Sciences.

CONFLICT OF INTEREST

The authors have no other relevant affiliations or financial involvement with any organization or entity with a financial interest in or financial conflict with the subject matter or materials discussed in the manuscript apart from those disclosed.

ORCID

Toktam Ghassemi https://orcid.org/0000-0002-6315-8134
Ali Moradi https://orcid.org/0000-0003-3866-0867

REFERENCES

Arai, S., & Orton, E. C. (2009). Immunoblot detection of soluble protein antigens from sodium dodecyl sulfate-and sodium deoxycholate-treated candidate bioscaffold tissues. *The Journal of Heart Valve Disease*, *18*, 439–443.

Badylak, S. F. (2007). The extracellular matrix as a biologic scaffold material. *Biomaterials*, *28*, 3587–3593.

Badylak, S. F., Freytes, D. O., & Gilbert, T. W. (2009). Extracellular matrix as a biological scaffold material: Structure and function. *Acta Biomaterialia*, *5*, 1–13. https://doi.org/10.1016/j.actbio.2008.09.013

Bahrami, A. R., Ebrahimi, M., Matin, M. M., Neshati, Z., Almohaddesin, M. R., Aghdami, N., & Bidkhori, H. R. (2011). Comparative analysis of chemokine receptor's expression in mesenchymal stem cells derived from human bone marrow and adipose tissue. *Journal of Molecular Neuroscience*, *44*, 178–185.

Benders, K., Boot, W., Cokelaere, S., Van Weeren, P., Gawlitta, D., Bergman, H., … Malda, J. (2014). Multipotent stromal cells outperform chondrocytes on cartilage-derived matrix scaffolds. *Cartilage*, *5*, 221–230. https://doi.org/10.1177/1947603514535245

Benders, K. E. M., Boot, W., Cokelaere, S. M., Weeren, P. R. V., Gawlitta, D., Bergman, H. J., … Malda, J. (2014). Multipotent stromal cells outperform chondrocytes on cartilage-derived matrix scaffolds. *Cartilage*, *5*(4), 1–10.

Bijlsma, J. W., Berenbaum, F., & Lafeber, F. P. (2011). Osteoarthritis: An update with relevance for clinical practice. *The Lancet*, *377*, 2115–2126. https://doi.org/10.1016/S0140-6736(11)60243-2

Blanco, F. J., & Ruiz-Romero, C. (2012). Osteoarthritis: Metabolomic characterization of metabolic phenotypes in OA. *Nature Reviews Rheumatology*, *8*, 130–132. https://doi.org/10.1038/nrrheum.2012.11

Chang, C.-H., Chen, C.-C., Liao, C.-H., Lin, F.-H., Hsu, Y.-M., & Fang, H.-W. (2014). Human acellular cartilage matrix powders as a biological scaffold for cartilage tissue engineering with synovium-derived mesenchymal stem cells. *Biomedical Materials Research*, *102A*, 2248–2257.

Conaghan, P. G. (2013). Osteoarthritis in 2012: Parallel evolution of OA phenotypes and therapies. *Nature Reviews Rheumatology*, *9*, 68–70. https://doi.org/10.1038/nrrheum.2012.225

Crapo, P. M., Gilbert, T. W., & Badylak, S. F. (2011). An overview of tissue and whole organ decellularization processes. *Biomaterials*, *32*, 3233–3243.

Elder, B. D., Eleswarapu, S. V., & Athanasiou, K. A. (2009). Extraction techniques for the decellularization of tissue engineered articular cartilage constructs. *Biomaterials*, *30*, 3749–3756.

Gilbert, T. W. (2012). Strategies for tissue and organ decellularization. *Cell Biochemistry*, *113*, 2217–2222.

Gilbert, T. W., Sellaro, T. L., & Badylak, S. F. (2006). Decellularization of tissues and organs. *Biomaterials*, *27*, 3675–3683.

Gong, Y. Y., Xue, J. X., Zhang, W. J., Zhou, G. D., Liu, W., & Cao, Y. (2011). A sandwich model for engineering cartilage with acellular cartilage sheets and chondrocytes. *Biomaterials*, *32*, 2265–2273.

Graham, M. E., Gratzer, P. F., Bezuhly, M., & Hong, P. (2016). Development and characterization of decellularized human nasoseptal cartilage matrix for use in tissue engineering. *The Laryngoscope*, *126*, 2226–2231. https://doi.org/10.1002/lary.25884

Grefrath, S. P., & Reynolds, J. A. (1974). The molecular weight of the major glycoprotein from the human erythrocyte membrane. *Proceedings of the National Academy of Sciences*, *71*, 3913–3916.

Henrotin, Y. (2014). Does signaling pathway inhibition hold therapeutic promise for osteoarthritis? *Joint, Bone, Spine*, *81*, 281–283. https://doi.org/10.1016/j.jbspin.2014.03.002

Im, O., Li, J., Wang, M., Zhang, L. G., & Keidar, M. (2012). Biomimetic three-dimensional nanocrystalline hydroxyapatite and magnetically synthesized single-walled carbon nanotube chitosan nanocomposite for bone regeneration. *International Journal of Nanomedicine*, *7*, 2087–2099.

Izadifar, Z., Chen, X., & Kulyk, W. (2012). Strategic design and fabrication of engineered scaffolds for articular cartilage repair. *Journal of Functional Biomaterials*, *3*, 799–838. https://doi.org/10.3390/jfb3040799

Jia, S., Liu, L., Pan, W., Meng, G., Duan, C., Zhang, L., … Liu, J. (2012). Oriented cartilage extracellular matrix-derived scaffold for cartilage tissue engineering. *Bioscience and Bioengineering*, *113*, 647–653. https://doi.org/10.1016/j.jbiosc.2011.12.009

Jorge-Herrero, E., Fernandez, P., De la Tone, N., Escudero, C., Garcia-Paez, J., Bujan, J., & Castillo-Olivares, J. (1994). Inhibition of the calcification of porcine valve tissue by selective lipid removal. *Biomaterials*, *15*, 815–820. https://doi.org/10.1016/0142-9612(94)90036-1

Kang, H., Peng, J., Lu, S., Liu, S., Zhang, L., Huang, J., … Guo, Q. (2014). In vivo cartilage repair using adipose-derived stem cell-loaded decellularized cartilage ECM scaffolds. *Tissue Engineering and Regenerative Medicine*, *8*, 442–453. https://doi.org/10.1002/term.1538

Kawazoye, S., Tian, S.-F., Toda, S., Takashima, T., Sunaga, T., Fujitani, N., … Matsumura, S. (1995). The mechanism of interaction of sodium dodecyl sulfate with elastic fibers. *Journal of Biochemistry*, *117*, 1254–1260. https://doi.org/10.1093/oxfordjournals.jbchem.a124852

Kheir, E., Stapleton, T., Shaw, D., Jin, Z., Fisher, J., & Ingham, E. (2011). Development and characterization of an acellular porcine cartilage bone matrix for use in tissue engineering. *Biomedical Materials Research*, *99A*, 283–294. https://doi.org/10.1002/jbm.a.33171

Knight, R., Wilcox, H., Korossis, S., Fisher, J., & INgham, E. (2008). The use of acellular matrices for the tissue engineering of cardiac valves. *Proceedings of the Institution of Mechanical Engineers, Part H: Journal of Engineering in Medicine*, *222*, 129–143.

Luo, L., Eswaramoorthy, R., Mulhall, K. J., & Kelly, D. J. (2016). Decellularization of porcine articular cartilage explants and their subsequent repopulation with human chondroprogenitor cells. *The Mechanical Behavior of Biomedical Materials*, *55*, 21–31.

Manek, N. J., & Lane, N. E. (2000). Osteoarthritis: Current concepts in diagnosis and management. *American Family Physician*, *61*, 1795–1804.

Marcacci, M., Filardo, G., & Kon, E. (2013). Treatment of cartilage lesions: What works and why? *Injury*, *44*, S11–S15. https://doi.org/10.1016/S0020-1383(13)70004-4

Mendoza-Novelo, B., & Cauich-Rodríguez, J. V. (2011). *Decellularization, stabilization and functionalization of collagenous tissues used as cardiovascular biomaterials*. London, UK: INTECH Open Access Publisher. https://doi.org/10.5772/25184

Moore, M., Sarntinoranont, M., & Mcfetridge, P. (2012). Mass transfer trends occurring in engineered ex vivo tissue scaffolds. *NIH*, *100A*, 2194–2203. https://doi.org/10.1002/jbm.a.34092

Moradi, A. 2015. Development of bovine cartilage extracellular matrix as a potential scaffold for chondrogenic induction of human dermal fibroblasts.pdf>. PhD, University of Malaya.

Moradi, A., Ataollahi, F., Sayar, K., Pramanik, S., Chong, P. P., Khalil, A. A., … Pingguan-Murphy, B. (2016). Chondrogenic potential of physically treated bovine cartilage matrix derived porous scaffolds on human dermal fibroblast cells. *Journal of Biomedical Materials Research Part A*, *104*, 243–254.

Moradi, A., Pramanik, S., Ataollahi, F., Abdul-Khalil, A., Kamarul, T., & Pingguan-Murphy, B. (2014). A comparison study of different physical treatments on cartilage matrix derived porous scaffolds for tissue engineering applications. *Science and Technology of Advanced Materials*, *15*, 065001. https://doi.org/10.1088/1468-6996/15/6/065001

Moradi, A., Pramanik, S., Ataollahi, F., Khalil, A. A., Kamarul, T., & Pingguan-Murphy, B. (2014). A comparison study of different physical treatments on cartilage matrix derived porous scaffolds for tissue engineering applications. *Science and Technology of Advanced Materials*, *15*, 1–12.

Muir, H. (1980). The chemistry of the ground substance of joint cartilage. *The joints and synovial fluid*, *2*, 27–94.

Peretti, G. M., Randolph, M. A., Villa, M. T., Buragas, M. S., & Yaremchuk, M. J. (2000). Cell-based tissue-engineered allogeneic implant for cartilage repair. *Tissue Engineering*, *6*, 567–576. https://doi.org/10.1089/107632700750022206

Platt, J. L., Fischel, R. J., Matas, A. J., Reif, S. A., Bolman, R. M., & Bach, F. H. (1991). Immunopathology of hyperacute xenograft rejection in a swine-to-primate model. *Transplantation*, *52*, 214–220. https://doi.org/10.1097/00007890-199108000-00006

Redman, S. N., Oldfield, S. F., & Archer, C. W. (2005). Current strategies for articular cartilage repair. *European Cells & Materials*, *9*, 23–32. https://doi.org/10.22203/eCM.v009a04

Reing, J. E., Brown, B. N., Daly, K. A., Freund, J. M., Gilbert, T. W., Hsiong, S. X., … Wolf, M. T. (2010). The effects of processing methods upon mechanical and biologic properties of porcine dermal extracellular matrix scaffolds. *Biomaterials*, *31*, 8626–8633.

Rémi, E., Meddahi-Pelle, A., Roques, C., Letourneur, D., Lansac, E., Medjahed-Hamidi, F., … Khelil, N. (2011). *Pericardial processing: Challenges, outcomes and future prospects*. London, UK: INTECH Open Access Publisher.

Rowland, C. R., Colucci, L. A., & Guilak, F. (2016). Fabrication of anatomically-shaped cartilage constructs using decellularized cartilage-derived matrix scaffolds. *Biomaterials*, *91*, 57–72.

Saarakkala, S., Rieppo, L., Rieppo, J., & Jurvelin, J. S. (2010). Fourier transform infrared (FTIR) microspectroscopy of immature, mature and degenerated articular cartilage. *Microscopy: Science, Technology, Applications and Education*, *1*, 403–414.

Schmitz, N., Laverty, S., Kraus, V., & Aigner, T. (2010). Basic methods in histopathology of joint tissues. *Osteoarthritis and Cartilage*, *18*, S113–S116. https://doi.org/10.1016/j.joca.2010.05.026

Schwarz, S., Koerber, L., Elsaesser, A. F., Goldberg-Bockhorn, E., Seitz, A. M., Dürselen, L., … Rotter, N. (2012). Decellularized cartilage matrix as a novel biomatrix for cartilage tissue-engineering applications. *Tissue Engineering Part A*, *18*, 2195–2209.

Sutherland, A. J., Beck, E. C., Dennis, S. C., Converse, G. L., Hopkins, R. A., Berkland, C. J., & Detamore, M. S. (2015). Decellularized cartilage may be a chondroinductive material for osteochondral tissue engineering. *PLoS ONE*, *10*(5), e0121966.

Sutherland, A. J., Converse, G. L., Hopkins, R. A., & Detamore, M. S. (2015). The bioactivity of cartilage extracellular matrix in articular cartilage regeneration. *Advanced Healthcare Materials*, *4*, 29–39. https://doi.org/10.1002/adhm.201400165

Toolan, B. C., Frenkel, S. R., Pereira, D. S., & Alexander, H. (1998). Development of a novel osteochondral graft for cartilage repair. *Biomedical Materials Research*, *41*, 244–250.

Valiani, A., Hashemibeni, B., Esfandiary, E., Ansar, M. M., Kazemi, M., & Esmaeili, N. (2014). Study of carbon nano-tubes effects on the chondrogenesis of human adipose derived stem cells in alginate scaffold. *International Journal of Preventive Medicine*, *5*(7), 825–834.

Yang, Q., Peng, J., Guo, Q., Huang, J., Zhang, L., Yao, J., … Lu, S. (2008). A Cartilage ECM-derived 3-D porous acellular matrix scaffold for in vivo cartilage tissue engineering with PKH26-labeled chondrogenic bone marrow-derived mesenchymal stem cells. *Biomaterials*, *29*, 2378–2387. https://doi.org/10.1016/j.biomaterials.2008.01.037

Yang, Z., Shi, Y., Wei, X., He, J., Yang, S., Dickson, G., … Li, G. (2010). Fabrication and repair of cartilage defects with a novel acellular cartilage matrix scaffold. *Tissue Engineering*, *16*, 865–876. https://doi.org/10.1089/ten.tec.2009.0444

Zheng, X., Lu, S., Zhang, W., Liu, S., Huang, J., & Guo, Q. (2011). Mesenchymal stem cells on a decellularized cartilage matrix for cartilage tissue engineering. *Biotechnology and Bioprocess Engineering*, *16*, 593–602. https://doi.org/10.1007/s12257-010-0348-9

How to cite this article: Ghassemi T, Saghatoleslami N, Mahdavi-Shahri N, Matin MM, Gheshlaghi R, Moradi A. A comparison study of different decellularization treatments on bovine articular cartilage. *J Tissue Eng Regen Med*. 2019;13:1861–1871. https://doi.org/10.1002/term.2936